

Crowding induces entropically-driven changes to DNA dynamics that depend on crowder structure and ionic conditions

Warren M. Mardoum¹, Stephanie M. Gorczyca¹, Kathryn E. Regan¹, Tsai-Chin Wu¹, and Rae M. Robertson-Anderson*¹

¹Department of Physics and Biophysics, University of San Diego, San Diego, CA, 92110, USA

*Correspondence: randerson@sandiego.edu

Keywords: macromolecular crowding, DNA diffusion, DNA conformation, single-molecule tracking, depletion interactions, fluorescence microscopy, DNA Compaction, entropic forces

Abstract

Macromolecular crowding plays a principal role in a wide range of biological processes including gene expression, chromosomal compaction, and viral infection. However, the impact that crowding has on the dynamics of nucleic acids remains a topic of debate. To address this problem, we use single-molecule fluorescence microscopy and custom particle-tracking algorithms to investigate the impact of varying macromolecular crowding conditions on the transport and conformational dynamics of large DNA molecules. Specifically, we measure the mean-squared center-of-mass displacements, as well as the conformational size, shape, and fluctuations, of individual 115 kbp DNA molecules diffusing through various *in vitro* solutions of crowding polymers. We determine the role of crowder structure and concentration, as well as ionic conditions, on the diffusion and configurational dynamics of DNA. We find that branched, compact crowders (10 kDa PEG, 420 kDa Ficoll) drive DNA to compact, whereas linear, flexible crowders (10 kDa, 500 kDa dextran) cause DNA to elongate. Interestingly, the extent to which DNA mobility is reduced by increasing crowder concentrations appears largely insensitive to crowder structure (branched vs linear), despite the highly different configurations DNA assumes in each case. We also characterize the role of ionic conditions on crowding-induced DNA dynamics. We show that both DNA diffusion and conformational size exhibit an emergent non-monotonic dependence on salt concentration that is not seen in the absence of crowders.

1 Introduction

Biological cells are highly crowded by macromolecules of varying sizes and structures. This complex crowded environment has been shown to directly impact key DNA processes and functions including replication, transcription, transformation, gene expression, and chromosomal compaction [1-6]. Investigating the impact of crowding on DNA is further motivated by the design of gene therapy and drug delivery systems, as well as the production and manipulation of synthetic cells and nanomaterials [2, 3, 7, 8]. Crowding can induce changes in DNA conformations, such as compaction, swelling, and elongation; and alter its diffusivity and intramolecular fluctuations [9-11]. However, the exact effect that crowding has on DNA mobility and conformation remains poorly understood. The wide range of differing results presented in the literature likely stems from the myriad of sizes and types of crowders, as well as the varying ionic conditions, used in *in vitro* experiments – both of which directly impact the effect of crowding on DNA.

Because crowding studies are largely motivated by the role crowding plays in cells, several studies have investigated DNA dynamics *in vivo* [1, 5, 12-14]. While these studies can directly illuminate DNA behavior in cells, the role that each variable (e.g., crowder size, structure, concentration, ionic condition) plays in the measured dynamics is hard to discern. Thus, researchers have turned to *in vitro* studies to methodically explore the role of each variable separately [1, 15, 16]. Most *in vitro* crowding studies use synthetic polymers, similar in size to the majority of small proteins in cells, at concentrations similar to those found in cells (20 – 40% w/v). Polysaccharides, such as dextran, polyethylene glycol (PEG) and Ficoll, are advantageous as crowders because they are inert, nonbinding, commercially available in a range of molecular weights, and can often be described by basic polymer theory [17-23]. While these crowders are often used interchangeably to mimic cellular crowding, they differ considerably in their structure and conformational shape.

Dextran is a linear, flexible polymer which is reported to assume a random coil conformation in solution with an empirical scaling of hydrodynamic radius with molecular weight of $R_h \sim M_w^{0.49}$ [20, 24, 25]. While this scaling exponent is close to that of an ideal polymer chain (scaling exponent of 0.5), dextran coils have been shown to be highly asymmetric [20]. At high concentrations, dextran can form entanglements more easily than branched crowders of similar molecular weight due to its linear, flexible structure. Further, its asymmetric shape suggests that at high enough concentrations nematic ordering is also more readily accessible than for branched crowders [26]. PEG is a flexible linear polymer with a hydrodynamic radius that scales as $R_h \sim M_w^{0.56}$. However, at concentrations

Crowding-induced changes to DNA dynamics that depend on crowder structure and ionic conditions

above ~7% w/v it self-associates to form highly branched structures which are suggested to behave more like hard spheres than random coils [27]. Ficoll is a highly-branched polymer that assumes a compact spherical conformation that can be described by the empirical scaling $R_h \sim M_w^{0.43}$ [19, 21].

A number of previous studies have examined the effects of these crowders on polymer transport, conformation, and stability [28-37]. However, the role these crowders play in the diffusion or conformation of large DNA molecules remains largely unexplored. Further, no previous studies have directly compared the impact that each of these distinctly-shaped crowders has on DNA dynamics. One previous study investigated the role of crowder shape on protein diffusion by measuring the diffusion of heart-shaped BSA and Y-shaped IgG proteins in crowded solutions of either BSA or IgG [38]. Results showed that the varying excluded volume resulting from the differently-shaped proteins played the most important role in diffusion, as opposed to crowder concentration or direct interactions. A previous simulation study examined the effect of crowder shape on the conformation of stiff rod polymers [26]. Results showed that at high concentrations, spherical crowders caused compaction of the polymers, reducing their radius of gyration R_g , while spherocylindrical particles increased R_g . The increase in R_g was thought to be caused by nematic ordering of spherocylindrical particles which allow the polymers to elongate in the direction of ordering.

We previously measured the diffusion and conformational dynamics of DNA crowded by dextran of varying molecular weights and concentrations [39, 40]. We found that the decrease in DNA diffusivity with increasing dextran concentration was actually less than expected based on the increasing viscosity of the crowding solutions [39]. Namely, measured diffusion coefficients followed a weaker scaling with viscosity than the classical Stokes-Einstein scaling $D \sim \eta^{-1}$. This “enhanced” diffusion was coupled with conformational elongation of DNA from its dilute random coil configuration.

While entropically-driven depletion interactions tend to compact large macromolecules to maximize the available volume for the small crowders, elongation or swelling could ensue if energetic or enthalpic effects counteract depletion forces. Because DNA is negatively charged, entropy maximization competes with the electrostatic cost of compaction, which can lead DNA to preferentially elongate rather than compact to reduce its conformational volume in certain cases. However, varying the ionic conditions of the solution can directly tune the electrostatic cost of compaction via positive ions (e.g., Na^+) screening DNA charge. In fact, increased salt concentrations have been shown to be essential to PEG-induced condensation/aggregation of DNA (known as Ψ -

Crowding-induced changes to DNA dynamics that depend on crowder structure and ionic conditions

compaction) [34, 35, 41, 42]. Since the discovery of Ψ -compaction [41], there have been numerous experimental [4, 6, 8, 42-52] and theoretical [53-59] studies investigating this phenomenon. Experiments have shown that Ψ -compaction of 166 kbp DNA is a first-order transition from random coil configurations to compacted states; and when the concentration and/or molecular weight of PEG is increased the required NaCl concentration for compaction is reduced [42]. The lowest reported NaCl concentration to induce compaction was 50 mM, which required 25% w/v of 11.5 kDa PEG, in contrast to the 300 mM NaCl required when 10% w/v of 3 kDa PEG was used. Magnetic and optical tweezers studies have examined the force required to uncoil compacted 48.5 kbp DNA in the presence of 15-30% w/v PEG and varying concentrations of NaCl [35, 44]. These studies found that this force increased as the PEG molecular weight and NaCl concentration increased (up to 6 kDa PEG and 2 M NaCl). The remaining studies on DNA compaction have focused on the effects of salt in confined conditions [6, 43, 60-64] or in the presence of charged crowders [65-72]. These previous studies have shed important new light on the role that charge screening plays in crowding-induced DNA compaction. However, the interplay between crowder shape and salt concentration has been left completely unexplored. Further, these studies have all focused on steady-state DNA conformations, so the question of how ionic strength impacts the mobility and conformational fluctuations of crowded DNA remains an important open question.

Here, we explore the effect of crowder shape and ionic conditions on the intriguing crowding-induced DNA dynamics that have previously been reported. Specifically, we track the center-of-mass mean-squared displacements, as well as the size and shape of single DNA molecules diffusing in solutions of crowders with varying structural properties and molecular weights (10 kDa dextran, 500 kDa dextran; 10 kDa PEG, 420 kDa Ficoll). Based on the literature, throughout the text we classify PEG and Ficoll as branched crowders and dextrans as linear crowders. We further explore the effect of salt concentration on the measured DNA properties by examining cases of 5-fold increased and decreased NaCl under maximally crowded conditions. We show that crowding-induced DNA conformations are highly-dependent on crowder structure, with branched crowders compacting DNA while linear crowders induce elongation. We further show DNA diffusion exhibits a surprising non-monotonic dependence on salt concentration in crowded environments.

2 Methods and Materials

All experimental methods and computational analysis, briefly summarized below, are thoroughly described and verified in [39, 40, 73]. Linear 115 kbp DNA molecules are prepared through

Crowding-induced changes to DNA dynamics that depend on crowder structure and ionic conditions

replication of supercoiled bacterial artificial chromosomes in *Escherichia coli*, followed by extraction, purification and enzymatic linearization [40]. A trace amount of DNA is fluorescently labeled with YOYO-I (Thermo Scientific) and embedded in a solution of 0-40% w/v crowding polymers dissolved in aqueous buffer (10 mM Tris-HCl, 1 mM EDTA, 10 mM NaCl, 4% β -mercaptoethanol). The four different crowders used are: 10 kDa dextran (Sdex), 500 kDa dextran (Ldex), 420 kDa Ficoll, and 10 kDa PEG (all purchased from Sigma Aldrich). Unless indicated, NaCl concentration is 10 mM. The viscosity of each crowded solution was measured using optical tweezers microrheology as described previously [40, 74].

To determine the diffusion coefficients as well as the conformational size, shape and fluctuations of crowded DNA, single embedded DNA molecules were imaged for 30 seconds at 10 frames per second using a high-speed CCD camera on a Nikon A1R epifluorescence microscope with 60x objective. All presented data are for ensembles of >200 molecules. Using custom-written algorithms (Matlab), we track the center-of-mass (COM) position (x, y) , as well as the lengths of the major and minor axes (R_{max} and R_{min} , respectively) of each molecule over time. We calculate the COM mean-squared-displacement in the x and y directions ($\langle \Delta x^2 \rangle$, $\langle \Delta y^2 \rangle$) to determine the diffusion coefficient D via $\langle \Delta x^2 \rangle = \langle \Delta y^2 \rangle = 2Dt$. Error bars are calculated using bootstrapping for 1000 sub-ensembles [75]. We use R_{max} as a measure of conformational size and we quantify the degree of molecular elongation or asymmetry by comparing R_{max} to R_{min} . Finally, we determine the time-dependence and lengthscales of intramolecular state fluctuations by calculating the ensemble-averaged fluctuation range $f(t) = \langle |R_{max}(0) - R_{max}(t)| \rangle / \langle R_{max} \rangle$ for a given lag time t . $f(t)$ can be understood as the relative lengthscale (compared to the conformational size) over which a given molecule fluctuates or “breathes” between different conformational states during a time t .

3 Results and Discussion

3.1 Crowder Structure

We first examine the role of crowder structure on DNA diffusion and conformation. Figure 1 displays the dependence of measured DNA diffusion coefficients on crowder concentration and solution viscosity for the four different crowders. As shown, the diffusion coefficients, D , for all crowders decrease with increasing crowder concentration, as expected given the increasing viscosity, η , of crowded solutions. However, the mobility reduction does not scale with increasing viscosity as classically predicted by the Stokes-Einstein relation, $D = k_b T / 6\pi \eta R$. Instead, the scaling of D with η is shallower than η^{-1} with an average scaling for all crowders of $D \sim \eta^{-0.5}$. Only for the two highest Ldex

Crowding-induced changes to DNA dynamics that depend on crowder structure and ionic conditions

concentrations, does this enhanced diffusion effect begin to be suppressed, with diffusion values beginning to more closely align with Stokes-Einstein predictions. The viscosity at these concentrations are also much higher than those measured for the other crowders at the same concentrations. This effect is likely due to the linear dextran polymers forming entanglements. In contrast, branched crowders of similar molecular weight assume hard sphere conformations, preventing entanglements. Sdex also does not form entanglements because of its smaller size compared to Ldex. For reference, the hydrodynamic radius, R_h , of Sdex, Ldex, PEG and Ficoll are 2.2 nm, 15.5 nm, 3.2 nm, and 5.6 nm, respectively [17, 19, 20, 25]. The conformational size of Ldex in solution is $>3x$ larger than the other crowders despite being similar molecular weight to Ficoll, thereby promoting polymer overlap and entanglement. Another interesting result that can be seen in Figure 1B is the similarity between the viscosities of PEG and Ficoll at equal concentrations, as well as their effect on DNA diffusion, despite their large M_w difference and $\sim 2x$ difference in R_h . This result suggests that PEG is indeed self-associating and forming branched structures which more closely mimic the branched structure and size of Ficoll. We note that the enhanced diffusion effect is more pronounced for linear crowders (SDex, Ldex) than branched crowders (PEG, Ficoll), which likely arises from differences in the crowding-induced DNA conformations which we describe below.

We previously attributed enhanced diffusion to conformational changes, which reduce the effective volume of the DNA [39, 40]. To build on this assumption and determine the role that crowder structure plays in conformational changes, we look to the measured major and minor axis lengths R_{max} and R_{min} . Figure 2(A-D) shows the distributions of DNA major axis lengths for each crowder type and concentration. There is a noticeable difference between the distributions for branched crowders compared to linear crowders. While branched crowders reduce R_{max} (narrowing distributions and shifting them to the left), linear crowders tend to increase R_{max} (widening and shifting distributions to the right).

To quantify the degree to which the average major axis length $\langle R_{max} \rangle$ as well as the spread in the distributions (quantified by the standard deviation ΔR_{max}) vary with crowding, we plot $\langle R_{max} \rangle$ vs ΔR_{max} (Fig 2E). The difference between linear and branched crowders is evident: branched crowders decrease ΔR_{max} and $\langle R_{max} \rangle$, signifying compaction, while linear crowders tend to increase both quantities, indicating elongation or swelling. Further, elongated or swollen configurations access a wider range of states (larger ΔR_{max}) than dilute condition random coil states, while the range of

Crowding-induced changes to DNA dynamics that depend on crowder structure and ionic conditions

accessed states for compacted configurations is reduced. This reduction is indicative of ordered compaction, in which tight intramolecular packing causes the molecules to fluctuate between fewer states. We note that for Sdex R_{max} actually decreases slightly, but ΔR_{max} still increases appreciably and the distributions show a more pronounced large R_{max} tail compared to dilute conditions. Thus, we interpret this data as still demonstrating elongation or swelling rather than compaction. Finally, the $(\langle R_{max} \rangle, \Delta R_{max})$ data points for all crowders show no discernible trend with crowder concentration, with most data points for 10-40% w/v clustering together. These data indicate that the crowding-induced conformational changes are an all or nothing effect, similar to the discrete first-order phase transition observed in Ψ -compaction.

To delineate between symmetric swelling versus elongation (induced by linear crowders), and determine if compacted configurations (induced by branched crowders) are more ellipsoid or spherical in nature than dilute condition random coils, we compare R_{max} to R_{min} (Fig 2F). The larger the $R_{max}:R_{min}$ ratio, the more asymmetric the conformation is. As shown, dilute condition random coil configurations exhibit a $\sim 3:2$ aspect ratio, as previously predicted and shown [76, 77]. Conversely, compacted conformations induced by branched crowders are more spherical in nature, similar to hard spheres. Linear crowders, on the other hand, markedly increase $R_{max}:R_{min}$, signifying elongation rather than symmetric swelling.

Because the spread in our conformational state distributions (ΔR_{max}) vary for the different crowders, we investigated whether this spread is a result of a heterogeneous ensemble of DNA molecules each assuming a different static conformation, or whether the ensemble is fairly uniform but each molecule transitions between different states over time. To determine the extent to which single molecules transition or “breathe” between different conformational states over time, we measure the change in R_{max} for varying lag times t and normalize by $\langle R_{max} \rangle$. We refer to this quantity as the fluctuation range, $f(t) = \langle |R_{max}(0) - R_{max}(t)| \rangle / \langle R_{max} \rangle$. As shown in Figure 3(A,B), $f(t)$ increases over time for all cases and approaches a steady-state value, which we term the steady-state fluctuation range f_{ss} (Fig 3C). Thus the spread in the conformational state data (Fig 2) arises from single molecules breathing between different states over time, rather than a heterogeneous ensemble of static conformations. The results shown in Figure 3 also display a marked difference between linear and branched crowders: while Sdex and Ldex increase f_{ss} by $\sim 30\%$ from the dilute value, both PEG and Ficoll reduce f_{ss} to $\sim 50\%$ of the dilute value. These data validate our interpretation that elongated molecules access a broader range of conformational states compared to more rigid compact

Crowding-induced changes to DNA dynamics that depend on crowder structure and ionic conditions

configurations. It is also notable that while there is a stark difference between the effect of linear crowders versus branched crowders, the fluctuation length shows little dependence on the concentration or size of crowders. This result is similar to the discrete phase transition seen in Figure 2, and underlines the critical role that crowder structure plays in DNA dynamics.

The question remains as to why linear crowders elongate DNA while branched crowders lead to compaction. Both conformations reduce the effective volume the DNA takes up in solution by either stretching into a long thin strand or compacting down to an ordered sphere. This crowding-induced phase transition arises from entropically-driven depletion interactions with the crowders. Namely, the DNA is forced to reduce its configurational volume to maximize the volume, and thus the entropy, of the crowders. However, why does the preferred configuration depend on crowder structure? As described in the Introduction, dextrans assume highly asymmetric random coil configurations in solution, compared to the hard sphere configurations of Ficoll and self-associated PEG crowders. If the DNA configurational transitions are entropically-driven then the DNA should assume the shape that allows for the most efficient packing of crowders around the DNA to maximize their available volume. Therefore, the DNA should assume a configuration that most closely matches that of the crowders while still reducing its volume from random coil. A previous simulation study comparing the effects of spherical vs cylindrical crowders on the conformational size of short rigid DNA molecules showed that cylindrical crowders elongated DNA while spherical crowders more readily compacted DNA [26]. While these results cannot be directly compared to our study, as our DNA is much larger and more flexible, they suggest that asymmetric crowders promote elongation to maximize the packing efficiency and available volume of the crowders. This study also showed that the presence of the DNA led to local nematic ordering of the crowders around the DNA which in turn facilitated DNA elongation [26]. In contrast, branched crowders are spherical in nature so packing is most efficient when DNA is likewise spherical.

3.2 Ionic Conditions

We next turn to the role of salt concentration on DNA crowding by carrying out measurements in the presence of NaCl concentrations that are 5x higher and lower than our standard conditions (10 mM NaCl). Because our data show much more of a dependence on crowder structure than concentration, in these experiments we fixed our crowder concentration at 40% w/v. Figure 4A displays the measured diffusion coefficients for dilute and crowded conditions as a function of NaCl concentration. As shown, we see a surprising non-monotonic dependence of DNA mobility on

Crowding-induced changes to DNA dynamics that depend on crowder structure and ionic conditions

[NaCl] when crowded: DNA exhibits the fastest diffusion at 10 mM NaCl. This effect is not seen in the dilute case in which the diffusion coefficient decreases with increasing NaCl concentration.

At first glance, the dilute case is counterintuitive in and of itself because as NaCl concentration increases, the wormlike chain model for DNA predicts that the persistence length l_p should decrease [78]. This predicted dependence is due to Na^+ ions partially screening the negatively charged DNA backbone, reducing the repulsion between neighboring DNA segments and thereby making the DNA more flexible. According to the freely-jointed chain model for flexible polymers, increasing l_p , while keeping the overall polymer length L fixed, should increase the radius of gyration of the polymer through the scaling, $R_G \sim (L * l_p)^{1/2}$ [79, 80]. Increasing R_G (and thus R_h) should in turn reduce the diffusion coefficient in accordance with the Stokes-Einstein equation ($D \sim R_h^{-1}$). However, the Stokes-Einstein relation approximates polymers as hard spheres and ignores intramolecular fluctuations. As NaCl concentration increases, and the number of persistence lengths per chain likewise increases, the DNA becomes more flexible and has more conformational degrees of freedom. This increase in conformational degrees of freedom leads to increased intramolecular fluctuations, which can in turn lead to slower COM motion as thermal kicks are going more into internal DNA fluctuations and less into the motion of the molecule as a whole. This argument is supported by Figure 4B, which shows that the steady-state fluctuation range of DNA (f_{ss}) increases with increasing [NaCl] in dilute conditions. We also measured the spread in the major axis lengths (ΔR_{max}) and find that, in the absence of crowding, ΔR_{max} increases with increasing [NaCl], indicating that higher salt conditions lead to more conformational states (Fig 4C). Finally, we find that $\langle R_{max} \rangle$ is actually largest at high salt (50 mM) rather than low salt (2 mM) (Fig 4C), in contradiction with the classical scaling $R_G \sim (L * l_p)^{1/2}$, but in support of our measured dependence of D on [NaCl], assuming the scaling $D \sim R_h^{-1}$.

Upon crowding, branched crowders induce greater DNA compaction and lead to smaller f_{ss} values compared to linear crowders for all salt conditions (Fig 4B). Thus, the effects of crowder structure on DNA conformation (described in the previous section) appear robust to environmental conditions. However, we do find that salt concentration plays a strong role on DNA conformations induced by all crowders. High salt conditions (50 mM NaCl) enable all crowders to markedly suppress conformational fluctuations of DNA (seen as a large drop in f_{ss} and ΔR_{max} , Fig 4B,C) and compact DNA (seen as a large drop in $\langle R_{max} \rangle$ and $\langle R_{min} \rangle$, Fig 4D) to maximize their entropy. This large change is facilitated by the increased flexibility of DNA at high [NaCl]. Because DNA is more flexible it can more easily transition between different conformational states, so it can more readily

Crowding-induced changes to DNA dynamics that depend on crowder structure and ionic conditions

undergo large entropically-driven changes to its conformation. This effect is in accord with the classic Ψ -compaction mechanism in which high salt conditions and crowding are both needed to efficiently induce bulk condensation of DNA [41]. In contrast, at the lowest NaCl concentration (2 mM) the steady-state fluctuation range remains nearly unchanged by crowders (Fig 4B). Low [NaCl] conditions also result in the smallest change to the conformational size of DNA, with DNA undergoing slight compaction in the presence of all crowder types (Fig 4D).

The question remains as to why the diffusion exhibits a non-monotonic dependence on [NaCl] when crowded. While 50 mM NaCl induces that largest change in DNA size from its dilute value, the most compacted and elongated DNA states are actually seen in 10 mM NaCl. As shown in Figure 4(C,D), the 10 mM NaCl data points lie at the extreme left and right-hand sides of the phase plots (low and high $\langle R_{max} \rangle$ values) while the 2 mM and 50 mM NaCl data are mostly clustered together in the middle of the plot. As our previous data suggested [39, 40], these extreme conformational state changes are what enables DNA to move faster than expected among crowders.

4 Conclusion

We have investigated the role of crowder structure, size and concentration, as well as ionic conditions, on the diffusion and conformational dynamics of large DNA molecules. We crowded 115 kbp DNA with widely used synthetic crowders that can be categorized into linear (dextrans) and branched (Ficoll, PEG) structures of small (10 kDa) and large (~500 kDa) molecular weights. We present a number of intriguing results that have not been previously predicted or observed, and cannot be explained by classical polymer theory. In all crowding conditions, we find that DNA diffuses faster than classically expected based on the increasing viscosity of the solutions, which we attribute to changes to the random coil conformation DNA assumes in dilute conditions. We find that DNA elongates in the presence of linear crowders while branched crowders compact DNA. Elongated conformations undergo larger conformational fluctuations than dilute random coils, while compacted configurations are more spherical and access a smaller range of conformational states. These findings are largely independent of crowder concentration and molecular weight. We also find that DNA dynamics exhibit a complex interplay between salt concentration and crowding. In dilute conditions, DNA diffusion decreases and the range of conformational states increases with increasing salt (from 2 mM to 50 mM NaCl). However, upon crowding, DNA diffusion and conformational changes exhibit an emergent non-monotonic dependence on salt concentration, with DNA diffusing the fastest and exhibiting the most extreme compaction or elongation in 10 mM NaCl compared to

lower and higher salt concentrations. Our collective results present several complex and unexpected phenomena that are highly relevant to polymer physics and cell biology alike. We hope that these results spur new theoretical investigations to fully understand these intriguing results.

5 Author Contributions

WMM prepared samples, collected data, analyzed data, interpreted data, wrote paper; SMG prepared samples, collected data, analyzed data; KR prepared samples, collected data; T-CW collected data, analyzed data; RMR-A designed experiments, analyzed data, interpreted data, wrote paper.

6 Funding

This research was funded by the Air Force Office of Scientific Research (Young Investigator Program Award No. FA95550-12-1-0315, Biomaterials Award No. FA9550-17-1-0249) and the National Institutes of Health (NNIGMS Award No. R15GM123420).

7 Conflict of Interest Statement

The authors declare no conflict of interest.

8 References

1. Ellis RJ. Macromolecular crowding: an important but neglected aspect of the intracellular environment. *Current opinion in structural biology* (2001) 11(1):114-9. PubMed PMID: 11179900.
2. Nakano S, Miyoshi D, Sugimoto N. Effects of molecular crowding on the structures, interactions, and functions of nucleic acids. *Chemical reviews* (2014) 114(5):2733-58. doi: 10.1021/cr400113m. PubMed PMID: 24364729.
3. Miyoshi D, Sugimoto N. Molecular crowding effects on structure and stability of DNA. *Biochimie* (2008) 90(7):1040-51. doi: 10.1016/j.biochi.2008.02.009. PubMed PMID: 18331845.
4. Tan C, Saurabh S, Bruchez MP, Schwartz R, LeDuc P. Molecular crowding shapes gene expression in synthetic cellular nanosystems. *Nature nanotechnology* (2013) 8(8):602-8.
5. Rivas G, Ferrone F, Herzfeld J. Life in a crowded world. *EMBO reports* (2004) 5(1):23-7.
6. Pelletier J, Halvorsen K, Ha B-Y, Paparcone R, Sandler SJ, Woldringh CL, et al. Physical manipulation of the Escherichia coli chromosome reveals its soft nature. *Proceedings of the National Academy of Sciences* (2012) 109(40):E2649-E56.
7. Heddi B, Phan AT. Structure of human telomeric DNA in crowded solution. *Journal of the American Chemical Society* (2011) 133(25):9824-33.
8. Li GW, Berg OG, Elf J. Effects of macromolecular crowding and DNA looping on gene regulation kinetics. *Nat Phys* (2009) 5(4):294-7. doi: Doi 10.1038/Nphys1222. PubMed PMID: WOS:000265264500021.

9. Zinchenko A. DNA conformational behavior and compaction in biomimetic systems: Toward better understanding of DNA packaging in cell. *Adv Colloid Interface Sci* (2016) 232:70-9. Epub 2016/03/16. doi: 10.1016/j.cis.2016.02.005. PubMed PMID: 26976700.
10. Nakano SI, Sugimoto N. Model studies of the effects of intracellular crowding on nucleic acid interactions. *Mol Biosyst* (2016) 13(1):32-41. Epub 2016/11/08. doi: 10.1039/c6mb00654j. PubMed PMID: 27819369.
11. Jorge AF, Nunes SCC, Cova TFGG, Pais AACC. Cooperative action in DNA condensation. *Current Opinion in Colloid & Interface Science* (2016) 26:66-74. doi: 10.1016/j.cocis.2016.09.014.
12. Lukacs GL, Haggie P, Seksek O, Lechardeur D, Freedman N, Verkman A. Size-dependent DNA mobility in cytoplasm and nucleus. *Journal of Biological Chemistry* (2000) 275(3):1625-9.
13. Regner BM, Vučinić D, Domnisoru C, Bartol TM, Hetzer MW, Tartakovsky DM, et al. Anomalous diffusion of single particles in cytoplasm. *Biophysical journal* (2013) 104(8):1652-60.
14. Platani M, Goldberg I, Lamond AI, Swedlow JR. Cajal body dynamics and association with chromatin are ATP-dependent. *Nature cell biology* (2002) 4(7):502-8.
15. Nakano S, Sugimoto N. Model studies of the effects of intracellular crowding on nucleic acid interactions. *Molecular Biosystems* (2017) 13(1):32-41. doi: 10.1039/c6mb00654j. PubMed PMID: WOS:000391697500003.
16. Minton AP. The influence of macromolecular crowding and macromolecular confinement on biochemical reactions in physiological media. *Journal of Biological Chemistry* (2001) 276(14):10577-80. doi: DOI 10.1074/jbc.R100005200. PubMed PMID: WOS:000167980900001.
17. Lee H, Venable RM, Mackerell AD, Jr., Pastor RW. Molecular dynamics studies of polyethylene oxide and polyethylene glycol: hydrodynamic radius and shape anisotropy. *Biophys J* (2008) 95(4):1590-9. Epub 2008/05/06. doi: 10.1529/biophysj.108.133025. PubMed PMID: 18456821; PubMed Central PMCID: PMC2483782.
18. Azri A, Privat M, Grohens Y, Aubry T. Linear rheological properties of low molecular weight polyethylene glycol solutions. *J Colloid Interface Sci* (2013) 393:104-8. Epub 2012/12/19. doi: 10.1016/j.jcis.2012.10.059. PubMed PMID: 23245885.
19. Fissell WH, Hofmann CL, Smith R, Chen MH. Size and conformation of Ficoll as determined by size-exclusion chromatography followed by multiangle light scattering. *Am J Physiol Renal Physiol* (2010) 298(1):F205-8. Epub 2009/10/23. doi: 10.1152/ajprenal.00312.2009. PubMed PMID: 19846572; PubMed Central PMCID: PMC2806116.
20. Venturoli D, Rippe B. Ficoll and dextran vs. globular proteins as probes for testing glomerular permselectivity: effects of molecular size, shape, charge, and deformability. *Am J Physiol Renal Physiol* (2005) 288(4):F605-13. Epub 2005/03/09. doi: 10.1152/ajprenal.00171.2004. PubMed PMID: 15753324.
21. Lavrenko PN, Mikryukova OI, SA D. Hydrodynamic properties and the shape of the molecules of the polysaccharide Ficoll-400 in solution. *Polymer Science USSR* (1986) 28(3): 576 -84.
22. Yun SI, Melnichenko YB, Wignall GD. Small-angle neutron scattering from symmetric blends of poly(dimethylsiloxane) and poly(ethylmethylsiloxane). *Polymer* (2004) 45(23):7969-77. doi: 10.1016/j.polymer.2004.09.050.

23. Ebagninin KW, Benchabane A, Bekkour K. Rheological characterization of poly(ethylene oxide) solutions of different molecular weights. *J Colloid Interface Sci* (2009) 336(1):360-7. Epub 2009/05/02. doi: 10.1016/j.jcis.2009.03.014. PubMed PMID: 19406425.
24. Luby-Phelps K, Castle PE, Taylor DL, Lanni F. Hindered diffusion of inert tracer particles in the cytoplasm of mouse 3T3 cells. *Proceedings of the National Academy of Sciences of the United States of America* (1987) 84(14):4910-3. PubMed PMID: 3474634; PubMed Central PMCID: PMC305216.
25. Armstrong JK, Wenby RB, Meiselman HJ, Fisher TC. The hydrodynamic radii of macromolecules and their effect on red blood cell aggregation. *Biophys J* (2004) 87(6):4259-70. Epub 2004/09/14. doi: 10.1529/biophysj.104.047746. PubMed PMID: 15361408; PubMed Central PMCID: PMCPMC1304934.
26. Kang H, Toan NM, Hyeon C, Thirumalai D. Unexpected Swelling of Stiff DNA in a Polydisperse Crowded Environment. *J Am Chem Soc* (2015) 137(34):10970-8. Epub 2015/08/13. doi: 10.1021/jacs.5b04531. PubMed PMID: 26267166.
27. Azri A, Giamarchi P, Grohens Y, Olier R, Privat M. Polyethylene glycol aggregates in water formed through hydrophobic helical structures. *J Colloid Interface Sci* (2012) 379(1):14-9. doi: 10.1016/j.jcis.2012.04.025. PubMed PMID: 22608144.
28. Nakano S-i, Karimata H, Ohmichi T, Kawakami J, Sugimoto N. The effect of molecular crowding with nucleotide length and cosolute structure on DNA duplex stability. *Journal of the American Chemical Society* (2004) 126(44):14330-1.
29. Gao M, Gnutt D, Orban A, Appel B, Righetti F, Winter R, et al. RNA Hairpin Folding in the Crowded Cell. *Angew Chem Int Edit* (2016) 55(9):3224-8. doi: 10.1002/anie.201510847. PubMed PMID: WOS:000370656200049.
30. Batra J, Xu K, Zhou HX. Nonadditive effects of mixed crowding on protein stability. *Proteins* (2009) 77(1):133-8. doi: 10.1002/prot.22425. PubMed PMID: 19408299; PubMed Central PMCID: PMC4456354.
31. Yang D, Khan S, Sun Y, Hess K, Shmulevich I, Sood AK, et al. Association of BRCA1 and BRCA2 Mutations With Survival, Chemotherapy Sensitivity, and Gene Mutator Phenotype in Patients With Ovarian Cancer EDITORIAL COMMENT. *Obstet Gynecol Surv* (2012) 67(3):164-5. PubMed PMID: WOS:000302177800015.
32. Dauty E, Verkman A. Actin Cytoskeleton as the Principal Determinant of Size-dependent DNA Mobility in Cytoplasm: a new barrier for non-viral gene delivery. *Journal of Biological Chemistry* (2005) 280(9):7823-8.
33. Szymanski J, Weiss M. Elucidating the origin of anomalous diffusion in crowded fluids. *Physical Review Letters* (2009) 103(3):038102.
34. Zinchenko AA, Yoshikawa K. Na⁺ shows a markedly higher potential than K⁺ in DNA compaction in a crowded environment. *Biophys J* (2005) 88(6):4118-23. doi: 10.1529/biophysj.104.057323. PubMed PMID: 15778438; PubMed Central PMCID: PMC1305642.
35. Cheng C, Jun-Li J, Shi-Yong R. Polyethylene glycol and divalent salt-induced RNA reentrant condensation revealed by single molecule measurements. *Soft Matter* (2015) 11:3927-35. doi: 10.1039/C5SM00619H.

36. Ramisetty SK, Dias RS. Synergistic role of DNA-binding protein and macromolecular crowding on DNA condensation. An experimental and theoretical approach. *J Mol Liq* (2015) 210:64-73. doi: 10.1016/j.molliq.2015.04.051. PubMed PMID: WOS:000363346700009.
37. Wegner AS, Wintraecken K, Spurio R, Woldringh CL, de Vries R, Odijk T. Compaction of isolated Escherichia coli nucleoids: Polymer and H-NS protein synergetics. *J Struct Biol* (2016) 194(1):129-37. doi: 10.1016/j.jsb.2016.02.009. PubMed PMID: WOS:000371193600014.
38. Balbo J, Mereghetti P, Herten DP, Wade RC. The shape of protein crowders is a major determinant of protein diffusion. *Biophys J* (2013) 104(7):1576-84. Epub 2013/04/09. doi: 10.1016/j.bpj.2013.02.041. PubMed PMID: 23561534; PubMed Central PMCID: PMC3617426.
39. Gorczyca SM, Chapman CD, Robertson-Anderson RM. Universal scaling of crowding-induced DNA mobility is coupled with topology-dependent molecular compaction and elongation. *Soft Matter* (2015) 11(39):7762-8. doi: 10.1039/c5sm01882j. PubMed PMID: 26303877.
40. Chapman CD, Gorczyca S, Robertson-Anderson RM. Crowding induces complex ergodic diffusion and dynamic elongation of large DNA molecules. *Biophys J* (2015) 108(5):1220-8. doi: 10.1016/j.bpj.2015.02.002. PubMed PMID: 25762333; PubMed Central PMCID: PMC4375539.
41. Lerman LS. A transition to a compact form of DNA in polymer solutions. *Proceedings of the National Academy of Sciences of the United States of America* (1971) 68(8):1886-90. PubMed PMID: 5288774; PubMed Central PMCID: PMC389314.
42. Vasilevskaya VV, Khokhlov AR, Matsuzawa Y, Yoshikawa K. Collapse of single DNA molecule in poly(ethylene glycol) solutions. *The Journal of Chemical Physics* (1995) 102(16):6595-602. doi: 10.1063/1.469375.
43. Zhang C, Shao P, van Kan J, JR vdM. Macromolecular crowding induced elongation and compaction of single DNA molecules confined in a nanochannel. *Proceedings of the National Academy of Sciences* (2009) 106(39):16651-6.
44. Ojala H, Ziedaite G, Wallin AE, Bamford DH, Haeggstrom E. Optical tweezers reveal force plateau and internal friction in PEG-induced DNA condensation. *European biophysics journal : EBJ* (2014) 43(2-3):71-9. doi: 10.1007/s00249-013-0941-x. PubMed PMID: 24477280.
45. Xu W, Muller SJ. Polymer-monovalent salt-induced DNA compaction studied via single-molecule microfluidic trapping. *Lab on a chip* (2012) 12(3):647-51. doi: 10.1039/c2lc20880f. PubMed PMID: 22173785; PubMed Central PMCID: PMC3322635.
46. Hirano K, Ichikawa M, Ishido T, Ishikawa M, Baba Y, Yoshikawa K. How environmental solution conditions determine the compaction velocity of single DNA molecules. *Nucleic acids research* (2012) 40(1):284-9. doi: 10.1093/nar/gkr712. PubMed PMID: 21896618; PubMed Central PMCID: PMC3245929.
47. Kawakita H, Uneyama T, Kojima M, Morishima K, Masubuchi Y, Watanabe H. Formation of globules and aggregates of DNA chains in DNA/polyethylene glycol/monovalent salt aqueous solutions. *J Chem Phys* (2009) 131(9):094901. doi: 10.1063/1.3216110. PubMed PMID: 19739867.
48. Saito T, Iwaki T, Yoshikawa K. DNA compaction induced by neutral polymer is retarded more effectively by divalent anion than monovalent anion. *Chemical Physics Letters* (2008) 465(1-3):40-4. doi: 10.1016/j.cplett.2008.09.040.

49. Maniatis T, Venable JH, Jr., Lerman LS. The structure of psi DNA. *Journal of molecular biology* (1974) 84(1):37-64. PubMed PMID: 4208607.
50. Minagawa K, Matsuzawa Y, Yoshikawa K, Khokhlov AR, Doi M. Direct Observation of the Coil-Globule Transition in DNA Molecules. *J Mol Biol* (1994) 84:37-64.
51. Yoshikawa K, Yoshikawa Y, Koyama Y, Kanbe T. Highly Effective Compaction of Long Duplex DNA Induced by Polyethelene Glycol with Pendant Amino Groups. *J Am Chem Soc* (1997) 119:6473-7.
52. Ramos JÉB, de Vries R, Ruggiero Neto J. DNA PSI-Condensation and Reentrant Decondensation: Effect of the PEG Degree of Polymerization. *J Phys Chem* (2005) 109:23661-5.
53. de Vries R. Flexible polymer-induced condensation and bundle formation of DNA and F-actin filaments. *Biophys J* (2001) 80(3):1186-94.
54. Post CB, H. ZB. Theory of DNA Condensation: Collapse Versus Aggregation *Biopolymers* (1982) 21:2123-37.
55. Grosberg AY, Y. EI, E. S. On the theory of PSI-condensation. *Biopolymers* (1982) 21:1487-501.
56. Post CB, Zimm BH. Internal condensation of a single DNA molecule. *Biopolymers* (1979) 18:1487-501.
57. Naghizadeh J, Massih AR. Concentration-Dependent Collapse of a Large Polymer. *Phys Rev Lett* (1978) 40:1299-303.
58. Shin J, Cherstvy AG, Metzler R. Polymer Looping Is Controlled by Macromolecular Crowding, Spatial Confinement, and Chain Stiffness. *Acs Macro Lett* (2015) 4(2):202-6. doi: 10.1021/mz500709w. PubMed PMID: WOS:000349814100013.
59. Shin J, Cherstvy AG, Metzler R. Kinetics of polymer looping with macromolecular crowding: effects of volume fraction and crowder size. *Soft Matter* (2014).
60. Zhang C, Gong Z, Guttula D, Malar PP, van Kan JA, Doyle PS, et al. Nanouidic compaction of DNA by like-charged protein. *The journal of physical chemistry B* (2012) 116(9):3031-6. doi: 10.1021/jp2124907. PubMed PMID: 22320240.
61. Jones JJ, van der Maarel JR, Doyle PS. Effect of nanochannel geometry on DNA structure in the presence of macromolecular crowding agent. *Nano letters* (2011) 11(11):5047-53. doi: 10.1021/nl203114f. PubMed PMID: 21988280.
62. Biswas N, Ichikawa M, Datta A, Sato YT, Yanagisawa M, Yoshikawa K. Phase separation in crowded micro-spheroids: DNA-PEG system. *Chemical Physics Letters* (2012) 539:157-62. doi: 10.1016/j.cplett.2012.05.033. PubMed PMID: WOS:000305802600031.
63. Negishi M, Sakaue T, Takiguchi K, Yoshikawa K. Cooperation between giant DNA molecules and actin filaments in a microsphere. *Phys Rev E* (2010) 81(5 Pt 1):051921. doi: 10.1103/PhysRevE.81.051921. PubMed PMID: 20866275.
64. Negishi M, Ichikawa M, Nakajima M, Kojima M, Fukuda T, Yoshikawa K. Phase behavior of crowded like-charged mixed polyelectrolytes in a cell-sized sphere. *Phys Rev E* (2011) 83(6). doi: Artn 06192110.1103/Physreve.83.061921. PubMed PMID: WOS:000292261900008.
65. de Vries R. Depletion-induced instability in protein-DNA mixtures: Influence of protein charge and size. *J Chem Phys* (2006) 125(1):014905. doi: 10.1063/1.2209683. PubMed PMID: 16863331.

Crowding-induced changes to DNA dynamics that depend on crowder structure and ionic conditions

66. de Vries R. DNA compaction by nonbinding macromolecules. *Polymer Science Series C* (2012) 54(1):30-5. doi: 10.1134/s1811238212070016.
67. Zinchenko A, Yoshikawa K. Compaction of double-stranded DNA by negatively charged proteins and colloids. *Current Opinion in Colloid & Interface Science* (2015) 20(1):60-5. doi: 10.1016/j.cocis.2014.12.005.
68. Ichiba Y, Yoshikawa K. Single chain observation on collapse transition in giant DNA induced by negatively-charged polymer. *Biochemical and biophysical research communications* (1998) 242(2):441-5. doi: 10.1006/bbrc.1997.7967. PubMed PMID: 9446814.
69. Kidoaki S, Yoshikawa K. Folding and unfolding of a giant duplex-DNA in a mixed solution with polycations, polyanions and crowding neutral polymers. *Biophysical chemistry* (1999) 76(2):133-43. PubMed PMID: 17027463.
70. Yoshikawa K, Hirota S, Makita N, Yoshikawa Y. Compaction of DNA Induced by Like-Charge Protein: Opposite Salt-Effect against the Polymer-Salt-Induced Condensation with Neutral Polymer. *J Phys Chem Lett* (2010) 1(12):1763-6. doi: 10.1021/jz100569e. PubMed PMID: WOS:000278963500003.
71. Zinchenko A, Tsumoto K, Murata S, Yoshikawa K. Crowding by Anionic Nanoparticles Causes DNA Double-Strand Instability and Compaction. *Journal of Physical Chemistry B* (2014) 118(5):1256-62. doi: 10.1021/jp4107712. PubMed PMID: WOS:000331153800009.
72. Barisik M, Atalay S, Beskok A, Qian SZ. Size Dependent Surface Charge Properties of Silica Nanoparticles. *J Phys Chem C* (2014) 118(4):1836-42. doi: 10.1021/jp410536n. PubMed PMID: WOS:000330610200010.
73. Laib S, Robertson RM, Smith DE. Preparation and characterization of a set of linear DNA molecules for polymer physics and rheology studies. *Macromolecules* (2006) 39(12):4115-9. doi: Doi 10.1021/Ma0601464. PubMed PMID: WOS:000238051600024.
74. Chapman CD, Lee K, Henze D, Smith DE, Robertson-Anderson RM. Onset of Non-Continuum Effects in Microrheology of Entangled Polymer Solutions. *Macromolecules* (2014) 47(3):1181-6. doi: Doi 10.1021/Ma401615m. PubMed PMID: WOS:000331344200036.
75. Efron B, Tibshirani R. *Statistical data analysis in the computer age*: University of Toronto, Department of Statistics (1990).
76. Haber C, Ruiz SA, Wirtz D. Shape anisotropy of a single random-walk polymer. *Proceedings of the National Academy of Sciences of the United States of America* (2000) 97(20):10792-5. doi: 10.1073/pnas.190320097. PubMed PMID: 10984514; PubMed Central PMCID: PMC27102.
77. Kuhn W. Über die Gestalt fadenförmiger Moleküle in Lösungen. *Kolloid-Zeitschrift* (1934) 68(1):2-15.
78. Marko JF, Siggia ED. Stretching DNA. *Macromolecules* (1995) 28:8759-70.
79. Rubinstein M, Colby RH. *Polymer physics*. Oxford ; New York: Oxford University Press (2003)..
80. Doi M, Edwards SF. *The theory of polymer dynamics*. Oxford Oxfordshire, New York: Clarendon Press; Oxford University Press (1987).

9 Figures and Captions

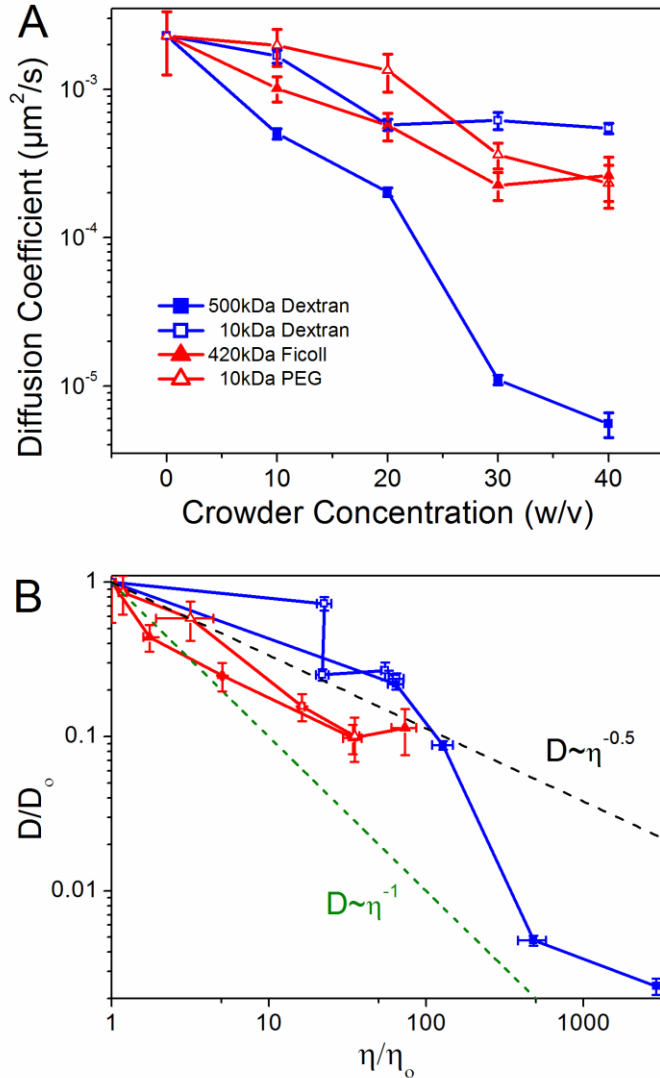


Figure 1: DNA diffusion decreases with increasing crowder concentrations, but universally diffuses faster than predicted by Stokes-Einstein scaling with viscosity. (A) Diffusion coefficients for DNA crowded by varying concentrations (w/v) of 500 kDa dextran (blue filled squares), 10 kDa dextran (blue open squares), 420 kDa Ficoll (red filled triangles) and 10 kDa PEG (red open triangles). (B) DNA diffusion coefficients, D , versus crowded solution viscosity, η , both normalized with respect to the corresponding dilute (0% crowding) values (D_0 , η_0). The dashed green line indicates the Stokes-Einstein relationship $D \sim \eta^{-1}$, while the black dashed line shows the average empirical scaling, $D \sim \eta^{-0.5}$. Note that nearly every D/D_0 value lies above the predicted Stokes-Einstein value.

Crowding-induced changes to DNA dynamics that depend on crowder structure and ionic conditions

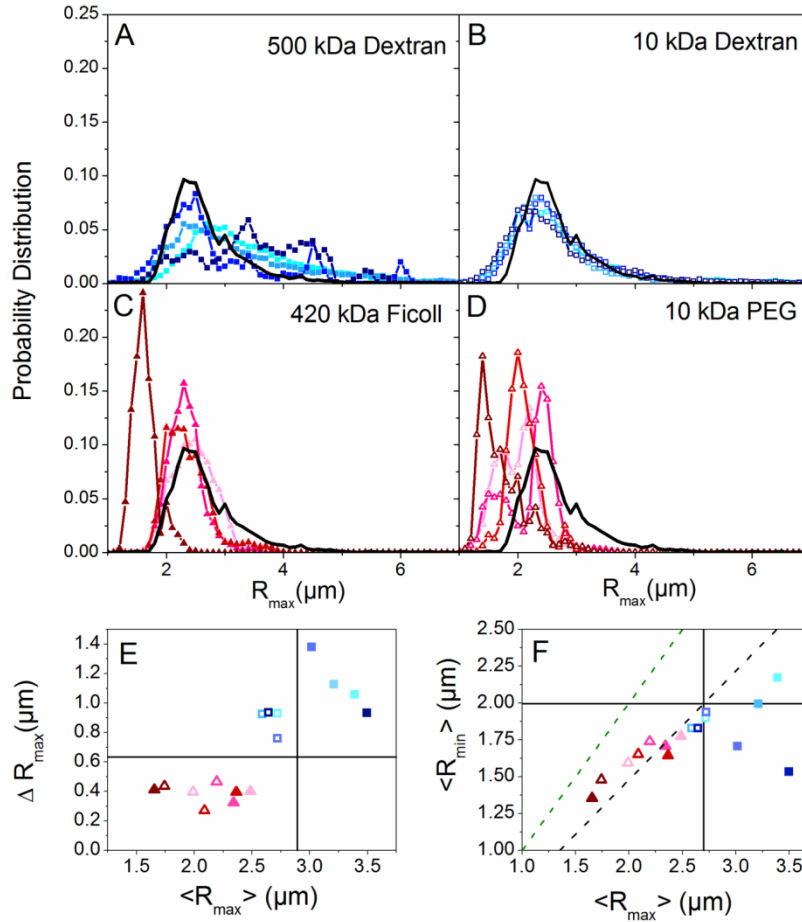


Figure 2: Crowding induces compaction or elongation of DNA dependent on the crowder structure. (A-D) Histograms of major axis lengths (R_{max}) for all crowding conditions compared to the dilute case (black line). Each panel displays results for a different crowder with blue hues denoting linear crowders (A,B; dextrans) and red hues indicating branched crowders (C,D; Ficoll, PEG). Closed symbols indicate high M_w crowders (A,C; 500 kDa dextran, 420 kDa Ficoll) and open symbols denote low M_w crowders (B,D; 10 kDa dextran, 10 kDa PEG). In each panel the color shade increases with increasing crowder concentration (10, 20, 30, 40% w/v). (E) The standard deviation of each R_{max} distribution, ΔR_{max} , versus the corresponding mean, $\langle R_{max} \rangle$. The color scheme is the same as A-D. The dilute value is indicated by the intersection of the horizontal and vertical lines. Symbols above or below the horizontal line indicate increased or decreased ranges in conformational states accessed, and symbols to the left or right of the vertical line indicate crowding-induced compaction or elongation. (F) Phase plot of the mean major and minor axis lengths ($\langle R_{max} \rangle, \langle R_{min} \rangle$) for each crowded condition. The green dashed line denotes the $\langle R_{max} \rangle : \langle R_{min} \rangle$ ratio for a spherical particle. The black dashed line denotes $\langle R_{max} \rangle : \langle R_{min} \rangle$ for the empirically measured dilute random coil configuration. Note that branched crowders (triangles) generally decrease $\langle R_{max} \rangle$ and $\langle R_{max} \rangle : \langle R_{min} \rangle$ indicating more spherical compacted conformations, while linear crowders (squares) tend to elongated DNA.

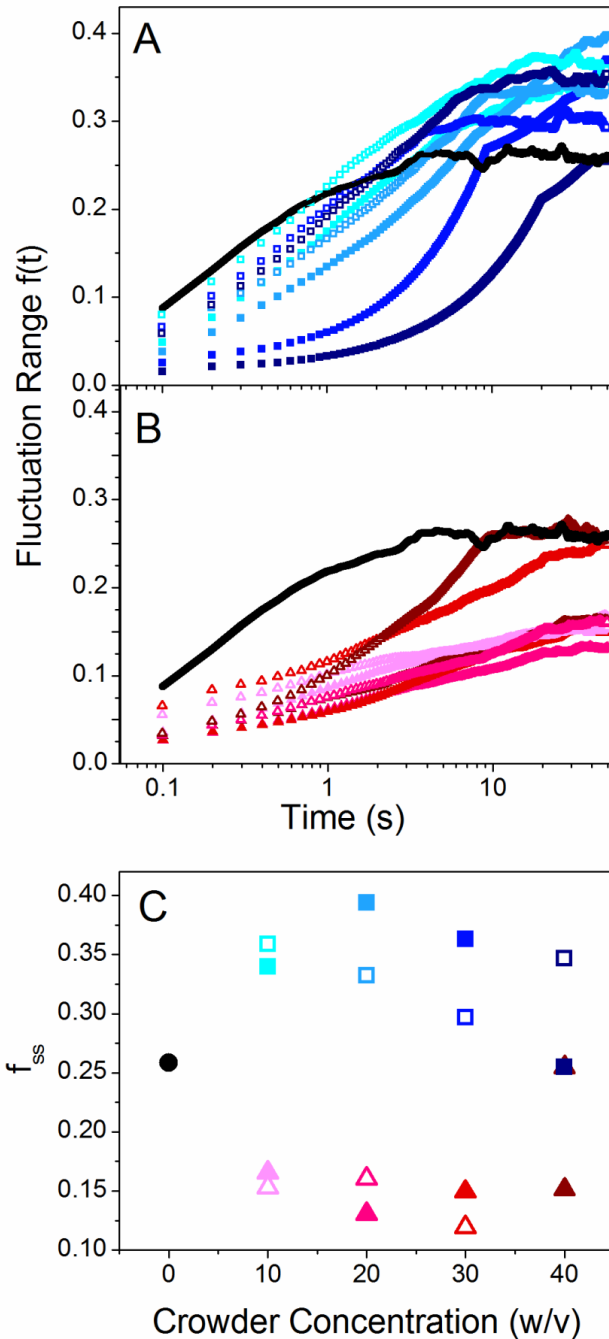


Figure 3: Crowded DNA molecules fluctuate over a range of different conformational states over time with a steady state fluctuation range that depends on crowder structure. (A,B) Fluctuation range, $f(t)$, as a function of time for linear (A) and branched (B) crowders compared to the dilute case (black lines). Open and closed symbols signify small (10 kDa) and large (~500 kDa) crowders and color shade increases with increasing crowder concentrations (10, 20, 30, 40% w/v). (C) Steady-state fluctuation range, f_{ss} (i.e. the terminal plateau values of $f(t)$), versus crowder concentration for linear (squares) and branched (triangles) crowders. As shown, linear crowders increase f_{ss} from the dilute value, while branched crowders reduce f_{ss} . These effects are largely independent of crowder size and concentration.

Crowding-induced changes to DNA dynamics that depend on crowder structure and ionic conditions

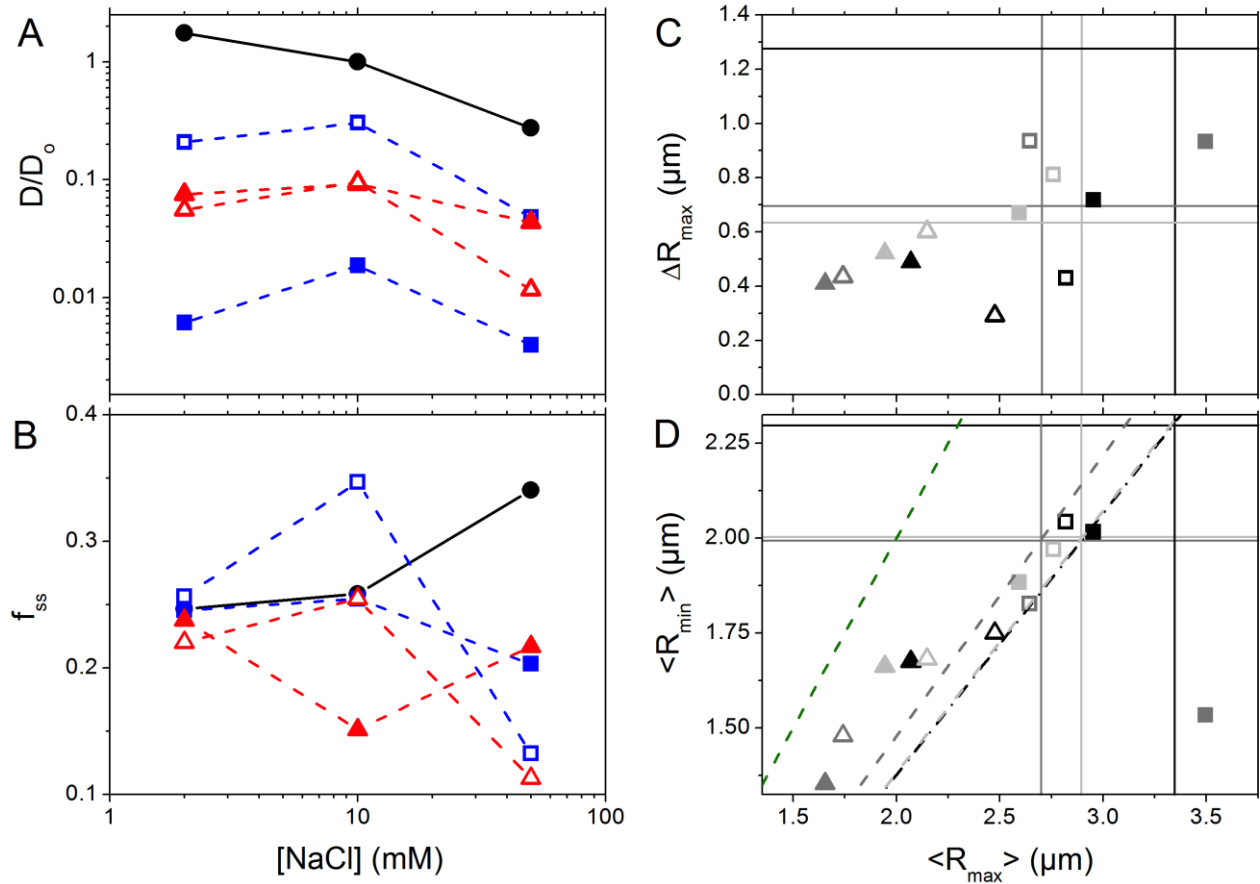


Figure 4: Diffusion and conformational dynamics of crowded DNA display unexpected non-monotonic dependence on NaCl concentration. (A) DNA diffusion coefficients, D , vs NaCl concentration for solutions with no crowders (black circles) and 40% w/v 500 kDa dextran (closed blue squares), 10 kDa dextran (open blue squares), 420 kDa Ficoll (closed red triangles) and 10 kDa PEG (open red triangles). Diffusion coefficients are normalized by the dilute D value at 10 mM NaCl (D_0). (B) Steady-state conformational fluctuation range of DNA, f_{ss} , as a function of [NaCl]. Color scheme is as in A. (C) Phase plot of the mean major axis length $\langle R_{max} \rangle$ and corresponding standard deviation ΔR_{max} for 10 kDa (open symbols) and ~ 500 kDa (closed symbols) linear (squares) and branched (triangles) crowders at NaCl concentrations of: 2 mM (light grey), 10 mM (grey), and 50 mM (black). The intersections of the color-coded horizontal and vertical lines denote the dilute values at the corresponding salt concentration. (D) Phase plot of the mean major and minor axis lengths ($\langle R_{max} \rangle, \langle R_{min} \rangle$) of crowded DNA. Colors and symbols are as in C. The dashed lines show the color-coded $\langle R_{max} \rangle : \langle R_{min} \rangle$ ratio (i.e. degree of sphericity) for the corresponding dilute DNA conformations. The green dashed line denotes the $\langle R_{max} \rangle : \langle R_{min} \rangle$ ratio for a spherical particle. As shown, 10 mM salt conditions lead to the most pronounced crowding-induced compaction and elongation (smallest and largest R_{max}) compared to lower or higher salt conditions.